Coverage and Energy Modeling of HetNet Under Base Station On-Off Model

Sida Song, Yongyu Chang, Xianling Wang, and Dacheng Yang

Small cell networks, as an important evolution path for next-generation cellular networks, have drawn much attention. Different from the traditional base stations (BSs) always-on model, we proposed a BSs on-off model, where a new, simple expression for the probabilities of active BSs in a heterogeneous network is derived. This model is more suitable for application in practical networks. Based on this, we develop an analytical framework for the performance evaluation of small cell networks, adopting stochastic geometry theory. We derive the system coverage probability; average energy efficiency (AEE) and average uplink power consumption (AUPC) for different association strategies; maximum biased received power (MaBRP); and minimum association distance (MiAD). It is analytically shown that MaBRP is beneficial for coverage but will have some loss in energy saving. On the contrary, MiAD is not advocated from the point of coverage but is more energy efficient. The simulation results show that the use of range expansion in MaBRP helps to save energy but that this is not so in MiAD. Furthermore, we can achieve an optimal AEE by establishing an appropriate density of small cells.

Keywords: Small cell, HetNet, base station on-off, association strategy, stochastic geometry, Poisson point process.

Manuscript received June 4, 2014; revised Nov. 26, 2014; accepted Dec. 9, 2014.

Sida Song (corresponding author, buptsongstar@gmail.com), Yongyu Chang (yychang@bupt.edu.cn), Xianling Wang (baggiorio18@gmail.com), and Dacheng Yang (yangdc@bupt.edu.cn) are with the Wireless Theory & Technology Laboratory (WT&T), the School of Information and Communications Engineering, Beijing University of Posts and Telecommunications, China.

I. Introduction

With the rapid growth in both data traffic in wireless communication and numbers of cellular network subscribers, it is becoming more and more difficult for conventional cellular systems to maintain minimum quality of service (QoS) requirements.

Densification of wireless cellular infrastructure through deployment of low-power access points (APs); that is, a heterogeneous network (HetNet), is a promising approach to meet increasing wireless traffic demands. A HetNet's network topology is composed of a diverse class of APs differing in transmit powers, radio access technologies, and backhaul capacities [1]. To meet the required capacity of a HetNet, many technologies will begin to emerge, as and when needed. Before their practical application, the performance of these new technologies must be assessed accurately; thus, new tractable models for their analysis and design are urgently needed. This paper focuses primarily on analyzing such HetNets.

By offloading wireless traffic from macro cells to small cells and decreasing the distance from users to base stations (BSs), small cell networks (SCNs) bring a multitude of benefits, including improved coverage, better user experiences, and more efficient spatial reuse of the frequency spectrum. Moreover, energy efficiency (EE) in cellular networks is becoming more and more of an important issue due to both the sharp rise in the cost of energy and the rise in carbon dioxide emissions [2].

This paper will focus on the coverage probability (CP) of HetNets, which is an important metric of a cellular network's performance.

In typical cellular networks, BSs use a significant portion of energy, reported to amount to about 60% to 80% [3]. Previous

works on EE mainly focused on a point-to-point link [4]–[5], while inter-cell interference was not modeled elaborately. In [6], EE in a cellular setting was investigated, whereby different cellular network architectures were compared mainly through system simulation. While evaluating network performance through system simulation can provide insights into some specific settings, the results cannot be extended to other scenarios, and the computational complexity is quite high. Fortunately, the utilization of stochastic geometry [7]–[8] to study cellular networks has been used extensively as an analytical tool with improved tractability. Recent works, [9]–[11], have shown that the modelling of a cellular network with BS locations drawn from a homogeneous Poisson point process (PPP) is as accurate as the traditional grid models when compared with a practical network deployment. Such modelling is a tractable approach for characterizing signal-to-interference ratio distributions.

Based on these reasons, this stochastic geometry tool is adopted to model the locations of BSs in this work. In addition, managing load or the number of users sharing the available resources per AP plays an important role in realizing capacity gains in HetNets. The load at an AP is dictated by the user-to-AP association strategy adopted in the network. Being able to analyze the impact of the load on the performance of systems is one of the goals of this paper. With the help of stochastic geometry, the optimal macro/micro BS density for energy-efficient HetNets with QoS constraints was analyzed in [12].

In the above works, it was assumed that each BS always had some user equipment (UE) to serve. We named the model associated with this assumption the traditional BSs always-on model. However, in a practical network, not all BSs are always active. This fact will affect the interference and subsequently the performance of the network. Such an interference effect becomes more prominent as the BS density increases, so much so that the UE density is comparable to the BS density, which is possible in small cell scenarios. So, in reality, a typical BS will have a certain probability of being active. This "BS active probability" is proposed in [13]. In [14], the author analyzes EE in SCNs using the probabilities of active BSs. However, [13]–[14] only focus on homogeneous networks. There is no formula in existence relating to the active probabilities of BSs in HetNets. In this work, we propose our BSs on-off model concerning the active probabilities of BSs in HetNets. Different from the BS sleeping mode [15] switching off the BS randomly, our model is based on the load of APs. Our approximation formula shows that the active probabilities of BSs in HetNets are related to UE density; that is, the ith tier AP density and the probability that a typical UE is associated with the ith tier.

In this paper, we describe our system model in Section II, where we introduce the following two different association strategies: maximum biased received power (MaBRP) and minimum association distance (MiAD). The BSs on-off model is proposed in Section III. Then the CP of a typical UE is derived in Section IV. After that, the average energy efficiency (AEE) and average uplink power consumption (AUPC) are analyzed in Section V. We present numerical results in Section VI to verify the validation of our proposed model. Finally, conclusions of our work are drawn in Section VII. Numerical results confirm that our BSs on-off model is more practical. Furthermore, the MaBRP is beneficial for coverage but will have some loss in energy saving. MiAD is not advocated from the point of coverage but is more energy efficient.

II. System Model

We consider a K-tier HetNet, which employs an orthogonal multiple access technique, as in that of the Orthogonal Frequency-Division Multiple Access in Long-Term Evolution. The BS active probability model is applied, which means that we are assuming that BSs are not always in an active state. Each tier's BSs are given according to an independent two-D homogeneous PPP, denoted as Φ_i, and which is of density λ_i, $i = 1, 2, \ldots, k$. Without loss of generality, an example of a two-tier HetNet comprising a macro tier and small cell tier is illustrated in Fig. 1. For a given PPP, the number of points in a bounded area is a Poisson-distributed random variable, and the points are uniformly distributed within the area. All the BSs in the network are of open access. The set of all tier-BS pairs in the network is denoted by $\Omega \triangleq \bigcup_{i=1}^{k} \bigcup_{j \in \Phi_i} (i, j)$. Furthermore, the users in the network are assumed to be distributed according to an independent 2-D homogenous PPP, Φ_u, of density λ_u.

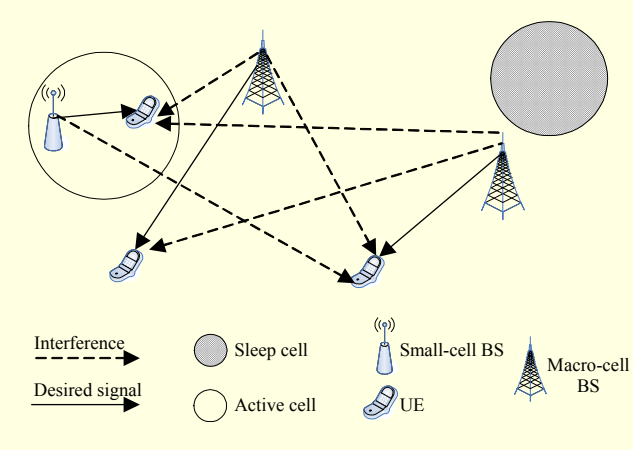

Fig. 1. Two-tier HetNet model with active and sleep cells.

We perform analysis on a typical UE located at the origin of the coordinate system by adding a user at the origin, which forms the process $\Phi_u \cup \{0\}$. This action is permitted through the use of Slivnyak's theorem [7], which states that the properties observed by a typical point of the PPP are the same as those observed by a point at the origin in the process $\Phi_u \cup \{0\}$.

To model the wireless channel, we consider a standard distance-based path loss with exponent $\alpha > 2$ along with Rayleigh fading. Hence, for a typical user, its received power from a BS in the ith tier is $P_i g r^{-\alpha}$, where P_i is the BS transmission power of the ith tier, $g \sim \exp(1)$, and r is the communication distance. We assume that all the UEs utilize a distance-proportional fractional power control of the form $P_u r^{\alpha\varepsilon}$, where P_u is the constant baseline transmission power of UE and $\varepsilon \in (0, 1)$ is the power control factor. Thus, as a UE connects to a new more distant serving BS, the transmission power increases, which is an important consideration for battery-powered mobile devices.

1. User Association and Resource Allocation

First, a general association metric is used, whereby a user is connected to a particular tier-BS pair, (m, k), if

$$(m,k) = \arg\max_{(i,j)\in\Omega} Z_i R_{ij}^{-\alpha}, \tag{1}$$

where R_{ij} denotes the distance of a typical user from the BS of (i,j), and Z_i is the association weight for the ith tier.

Two different kinds of user association strategies are discussed.

A. MaBRP

When $Z_i = P_i \beta_i$, the association strategy is the cell range expansion (CRE) technique. In this paper, we assume that BSs in the ith tier use the same bias factor, β_i.

B. MiAD

When $Z_i = 1$, a typical user is associated to the nearest BS. The association strategy will directly influence the load across the network. Both MaBRP and MiAD are illustrated in Fig. 2. The figure shows that more UEs will associate with high-power APs in MaBRP, but in MiAD, the result is different in that a more balanced network load is achieved instead. For notational brevity, we define the following:

$$\hat{Z}_j \triangleq \frac{Z_j}{Z_i}, \ \hat{P}_j \triangleq \frac{P_j}{P_i}, \text{ and } \hat{B}_j \triangleq \frac{B_j}{B_i}, \tag{2}$$

which characterize association weight ratio, transmit power ratio, and bias ratio, respectively.

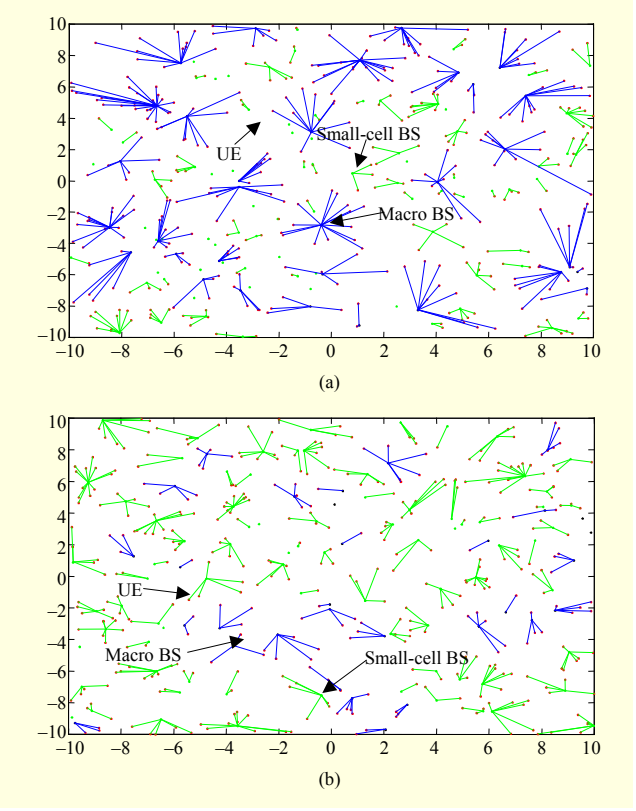

Fig. 2. BS association in two-tier HetNet: (a) MaBRP and (b) MiAD.

Lemma 1. The probability density function (PDF) of the distance R_s between a typical UE and its serving BS is given by

$$f_{R_s}(r) = \sum_{i=1}^{k} 2\pi\lambda_i r \exp(-\pi Q_i r^2), \tag{3}$$

where

$$Q_i = \sum_{j=1}^{k} \lambda_j \left(\hat{Z}_j\right)^{2/\alpha}. \tag{4}$$

Proof. The cumulative distribution function (CDF) of R_s can be expressed as

$$P\left(R_s < r\right) = \sum_{i=1}^{k} P\left(R_i < r, \text{UE access to } i\text{th tier}\right), \tag{5}$$

where R_i is the distance of the typical user from the nearest BS in the ith tier.

$$P(R_i < r, \text{UE access to } i\text{th tier}) \tag{6}$$

$$= \int_0^r P\left(Z_i R_i^{-\alpha} > \max_{\substack{j=1,2,\ldots,k \\ j\neq i}} Z_j R_j^{-\alpha}\right) f_{R_i}(r)\, \mathrm{d}r \tag{7}$$

$$= \int_0^r P\left(\bigcap_{\substack{j=1,2,\ldots,k \\ j\neq i}} \left\{Z_i R_i^{-\alpha} > Z_j R_j^{-\alpha}\right\}\right) f_{R_i}(r)\, \mathrm{d}r \tag{8}$$

$$\overset{(a)}{=}\int_0^r \prod_{\substack{j=1,2,\ldots,k \\ j\neq i}} P\left(R_j > \left(\hat{Z}_j\right)^{1/\alpha} r\right) f_{R_i}(r)\, \mathrm{d}r, \tag{9}$$

where the "(a)" in (9) follows from the independence of Φ_i. Now, the CDF of R_i and the probability $P(R_i > r)$ can be written as [9] with

$$f_{R_i}(r) = 2\pi\lambda_i r e^{-\pi\lambda_i r^2}, \tag{10}$$

$$P(R_i > r) = e^{-\pi\lambda_i r^2}. \tag{11}$$

So, substituting (10) and (11) into (9), we obtain

$$\begin{aligned} &P(R_i < r, \text{UE access to } i\text{th tier}) \\ &= 2\pi\lambda_i \times \int_0^r r \exp\left(-\pi \sum_{j=1,2,\ldots,k} \lambda_j \left(\hat{Z}_j\right)^{2/\alpha} r^2\right) \mathrm{d}r \end{aligned} \tag{12}$$

and $f_{R_s}(r) = \dfrac{\mathrm{d}\left[P(R_s < r)\right]}{\mathrm{d}r}$. Using (5) and (12), we obtain the desired results. ■

Lemma 1 confirms our basic intuition of the fact that the association strategy and density of BSs will influence the user association distance.

Lemma 2. The probability that a typical user is associated with the ith tier is

$$A_i = \frac{\lambda_i}{Q_i}. \tag{13}$$

Proof. The result can be proved by a minor modification of Lemma 1 of [10]; that is,

$$A_i = \mathrm{E}\left[P\left(Z_i R_i^{-\alpha} > \max_{\substack{j=1,2,\ldots,k \\ j\neq i}} Z_j R_j^{-\alpha}\right)\right] \tag{14}$$

$$= \int_0^\infty P\left(\bigcap_{\substack{j=1,2,\ldots,k \\ j\neq i}} \left\{Z_i R_i^{-\alpha} > Z_j R_j^{-\alpha}\right\}\right) f_{R_i}(r)\, \mathrm{d}r. \tag{15}$$

From almost the same process as Lemma 1 of this paper, we obtain

$$A_i = 2\pi\lambda_i \times \int_0^\infty r \exp\left(-\pi \sum_{j=1,2,\ldots,k} \lambda_j \left(\hat{Z}_j\right)^{2/\alpha} r^2\right) \mathrm{d}r. \tag{16}$$

With some simple mathematical derivation, we obtain the desired results. ■

From Lemma 2, we find that a user is more likely to connect to a tier with high BS density and high association weight Z_i.

We specifically focus on the data channels. When a BS has no UE to serve, all the frequency-time resource blocks (RBs) for data channels will be left blank, while the other BSs with at least one associated UE will occupy all the RBs for data transmissions. No intracell interference is incorporated, since we assume that orthogonal multiple access is employed among intracell UEs. Considering the characteristic of interference-limited in dense cellular networks, we ignore the effect of noise in the calculation of signal-to-interference-plus-noise ratio (SINR) in this paper. Furthermore, we utilize the full buffer traffic model for all the UEs. Best-effort traffic is assumed, and there is no quality or latency requirement for the traffic model. The available resources at each BS are assumed to be allocated evenly among all its UEs to simulate a round-robin scheduling of the highest level of fairness.

III. BS On-Off Model

In this paper, we switch off the BSs that have no users to serve. This will directly influence the interference of the whole network. Under the system model presented above, we obtain an approximation of the transmitting BS process by introducing the probability η_i of a typical ith-tier active BS, the BSs on-off model.

Lemma 3. The probability that a typical BS is active is given by

$$\eta_i = 1 - \left(1 + \frac{\lambda_u A_i}{3.5\lambda_i}\right)^{-3.5} \quad \text{for } i = 1, 2, \ldots, k. \tag{17}$$

Proof. Since a BS is inactive when there is no UE associated to it, we can obtain η_i using the following result from [11] that approximates the PDF of S_i; that is, the area of a typical BS of the ith tier in a Poisson random tessellation is

$$f_{S_i}(x) = \frac{3.5^{3.5}}{\Gamma(3.5)} \times \frac{\lambda_i}{A_i} \times \left(\frac{\lambda_i}{A_i} x\right)^{2.5} \times \exp\left(-3.5\frac{\lambda_i}{A_i} x\right). \tag{18}$$

So,

$$\eta_i = 1 - \int_0^\infty P(\text{no UE in area } x) f_{S_i}(x)\, \mathrm{d}x \tag{19}$$

$$\overset{(a)}{=} 1 - \int_0^\infty e^{-\lambda_u x} f_{S_i}(x)\, \mathrm{d}x \tag{20}$$

$$= 1 - \left(1 + \frac{\lambda_u A_i}{3.5\lambda_i}\right)^{-3.5} \quad \text{for } i = 1, 2, \ldots, k, \tag{21}$$

where the "(a)" in (20) follows from the void probability of the UE Poisson process in area x. ■

Lemma 3 confirms that a higher BS density leads to a lower η_i and a higher UE density results in a higher η_i. We also should note that the association strategy will influence η_i because of its relationship with A_i. Since the independent thinning of a PPP is still PPP [16], so given η_i, the transmitting BSs can be approximated as a PPP, $\tilde{\Phi}_i$, having density $\eta_i\lambda_i$.

IV. Downlink CP

In this section, we derive the CP of a typical UE under the system model; that is, the association strategy and BS on-off

model presented in Sections II and III, respectively. Given that a UE is associated with the *i*th tier, the CP of this UE is defined by

$$\mathcal{C}_i \triangleq \mathrm{E}\left[P\left(\mathrm{SINR}_i(r) \geq \tau\right)\right], \tag{22}$$

where $\mathrm{SINR}_i(r)$ is the SINR of this UE at a distance r from its associated BS, and τ is the SINR target. From the law of total probability, the CP, $\mathcal{C}$, of a typical UE is

$$\mathcal{C} = \sum_{i=1}^{k} \mathcal{C}_i A_i. \tag{23}$$

Considering the probabilities of the active BSs, as proposed in Lemma 3, we give Theorem 1 as follows:

Theorem 1. The CP of a typical UE associated with the *i*th tier is

$$\mathcal{C}_i = \frac{Q_i}{\mathcal{D}_i\left(\tau, \alpha, \{\eta_j\}\right)} \quad \text{for } i = 1, 2, \ldots, k, \tag{24}$$

where

$$\mathcal{D}_i\left(\tau, \alpha, \{\eta_j\}\right) = Q_i + \sum_{j=1}^{2} \eta_j \lambda_j (\hat{P}_j)^{2/\alpha} \cdot Z(\tau, \alpha, \Delta), \tag{25}$$

where

$$\Delta = \begin{cases} \hat{\beta}_j & \text{for MaBRP,} \\ \hat{P}_j^{-1} & \text{for MiAD;} \end{cases} \tag{26}$$

$$Z(a,b,c) = \frac{2ac^{(2/b)-1}}{b-2} {}_2F_1\left[1,\ 1-\frac{2}{b};\ 2-\frac{2}{b};\ -\frac{a}{c}\right]; \text{ and } {}_2F_1[\cdot]$$

denotes the Gauss hypergeometric function, which is defined by the power series ${}_2F_1[q,r;s;z] = \sum_{n=0}^{\infty} \frac{(q)_n (r)_n}{(s)_n} \frac{z^n}{n!}$, where, here, $(x)_n$ is the Pochhammer symbol, which is defined by

$$(x)_n = \begin{cases} 1 & n = 0, \\ x \times (x+1) \times \cdots \times (x+n-1) & n > 0. \end{cases}$$

Proof. From (22), the CP of the *i*th tier is given as

$$\mathcal{C}_i = \int_{r=0}^{\infty} P\left(\mathrm{SINR}_i(r) \geq \tau\right) f_{R_i}(r)\,\mathrm{d}r, \tag{27}$$

where $f_{R_i}(r)$ is the distance-PDF according to (10). By ignoring the effect of noise, $\mathrm{SINR}_i(r) = \left(P_i g r^{-\alpha}\right)/I$, where I is the interference power from the other transmitting BSs.

$$P\left(\mathrm{SINR}_i(r) \geq \tau\right) = P\left(\frac{P_i g r^{-\alpha}}{I} \geq \tau\right) \tag{28}$$

$$= P\left(g \geq \frac{\tau I}{P_i r^{-\alpha}}\right) \tag{29}$$

$$\overset{(a)}{=} \int_0^{\infty} \exp\left(-\frac{\tau I}{P_i r^{-\alpha}}\right) f_I(I)\,\mathrm{d}I \tag{30}$$

$$\overset{(b)}{=} \mathcal{L}_I\left(\frac{\tau}{P_i r^{-\alpha}}\right) \tag{31}$$

$$\overset{(c)}{=} \exp\left\{-\pi r^2 \sum_{j=1}^{k} \eta_j \lambda_j \left(\frac{P_j}{P_i}\right)^{2/\alpha} \times Z(\tau, \alpha, \Delta)\right\}, \tag{32}$$

where $\Delta = \begin{cases} \hat{\beta}_j & \text{for MaBRP,} \\ \hat{P}_j^{-1} & \text{for MiAD;} \end{cases}$ the "(a)" in (30) follows from $g \sim \exp(1)$; the "(b)" in (31) is obtained through a Laplace transform of I; and the "(c)" in (32) is obtained from [10] with a minor modification; that is, the density of interfering BSs in the *j*th tier is $\eta_j \lambda_j$ and considering different association strategies. The function $Z(\tau, \alpha, \Delta)$ is from

$$Z(a,b,c) = \frac{2ac^{(2/b)-1}}{b-2} {}_2F_1\left[1,\ 1-\frac{2}{b};\ 2-\frac{2}{b};\ -\frac{a}{c}\right]. \tag{33}$$

So, substituting (10) and (32) into (27), and with some simple mathematical derivation, we obtain the desired results. ■

Combining (13), (23), and (24), the CP of a typical UE is

$$\mathcal{C} = \sum_{i=1}^{k} \frac{\lambda_i}{\mathcal{D}_i\left(\tau, \alpha, \{\eta_j\}\right)}. \tag{34}$$

This metric represents the average fraction of the cell area that is in coverage at any time and is also exactly the complementary CDF (CCDF) of SINR over the entire network. The validation of Theorem 1 will be verified in Section VI.

V. EE and Uplink Power Consumption

First, we derive the AEE of a typical UE, and then the uplink power consumption model is proposed.

1. AEE

Before we define AEE, we first give the definition of the average rate (AR). The AR of a typical UE associated with the *i*th tier is the ergodic rate of a typical UE at a distance r from its serving BS, defined as

$$\bar{\mathcal{R}}_{\mathrm{ue}}^{i} \triangleq \mathrm{E}\left[\ln\left(1 + \mathrm{SINR}_i(r)\right)\right]. \tag{35}$$

EE is defined as the ratio of spectral efficiency to power consumption and is measured in the unit of nats/Hz/W. For a typical active BS, the transmission power is allocated uniformly for all its UEs. The cell load is approximated as follows.

Lemma 4. The average number of UEs associated with a BS in the *i*th tier is given by

$$\bar{N}_{\mathrm{ue}}^{i} = \frac{\lambda_{\mathrm{u}}}{Q_i} \quad \text{for } i = 1, 2, \ldots, k. \tag{36}$$

Proof. This result can be proved by a minor modification of Lemma 2 in [10]. ■

We focus on the AEE of a typical UE, which is given by

$$\mathrm{AEE}_{\mathrm{ue}}^{i} \triangleq \mathrm{E}\left[\frac{\ln\left(1+\mathrm{SINR}_i(r)\right)}{P_{\mathrm{ue}}^{i}}\right], \tag{37}$$

where $P_{\mathrm{ue}}^{i} = P_i / \bar{N}_{\mathrm{ue}}^{i}$ is the transmission power allocated to a typical UE that is associated with the *i*th tier. From the law of total probability, the AEE of a typical UE is

$$\mathrm{AEE}_{\mathrm{ue}} = \sum_{i=1}^{k} \mathrm{AEE}_{\mathrm{ue}}^{i} A_i. \tag{38}$$

Theorem 2. The AEE of a typical UE associated with the *i*th tier is

$$\mathrm{AEE}_{\mathrm{ue}}^{i} = Q_i \int_0^{\infty} \left[\mathcal{D}_i\left(e^{\tau P_i/\bar{N}_{\mathrm{ue}}^{i}} - 1, \alpha, \{\eta_j\}\right)\right] \mathrm{d}\tau. \tag{39}$$

Proof. From (37), the AEE of a typical UE associated with the *i*th tier is given as

$$\mathrm{AEE}_{\mathrm{ue}}^{i} = \int_{r=0}^{\infty} \mathrm{E}_{\mathrm{SINR}_i}\left[\frac{\ln\left(1+\mathrm{SINR}_i(r)\right)}{P_{\mathrm{ue}}^{i}}\right] f_{R_i}(r)\,\mathrm{d}r, \tag{40}$$

where $f_{R_i}(r)$ is the distance-PDF according to (10).

$$\begin{aligned} &\mathrm{E}_{\mathrm{SINR}_i}\left[\frac{\ln\left(1+\mathrm{SINR}_i(r)\right)}{P_{\mathrm{ue}}^{i}}\right] \\ &\overset{(a)}{=} \int_0^{\infty} P\left[\frac{\ln\left(1+\mathrm{SINR}_i(r)\right)}{P_{\mathrm{ue}}^{i}} > \tau\right] \mathrm{d}\tau, \end{aligned} \tag{41}$$

where the "(a)" in (41) follows $\mathrm{E}[X] = \int_0^{\infty} P[X > x]\,\mathrm{d}x$ for $X > 0$.

The rest of the derivation is almost the same as the proof of Theorem 1.

$$P\left[\frac{\ln\left(1+\mathrm{SINR}_i(r)\right)}{P_{\mathrm{ue}}^{i}} > \tau\right]$$

$$= P\left(\frac{P_i g r^{-\alpha}}{I} \geq e^{\tau P_{\mathrm{ue}}^{i}} - 1\right) \tag{42}$$

$$= P\left(g \geq \frac{(e^{\tau P_{\mathrm{ue}}^{i}} - 1) I}{P_i r^{-\alpha}}\right) \tag{43}$$

$$= \int_0^{\infty} \exp\left(-\frac{(e^{\tau P_{\mathrm{ue}}^{i}} - 1) I}{P_i r^{-\alpha}}\right) f_I(I)\,\mathrm{d}I \tag{44}$$

$$= \mathcal{L}_I\left(\frac{(e^{\tau P_{\mathrm{ue}}^{j}} - 1)}{P_j r^{-\alpha}}\right) \tag{45}$$

$$= \exp\left\{-\pi r^2 \sum_{j=1}^{k} \eta_j \lambda_j \left(\frac{P_j}{P_i}\right)^{2/\alpha} \cdot Z(e^{\tau P_{\mathrm{ue}}^{j}} - 1, \alpha, \Delta)\right\}. \tag{46}$$

So, substituting (13) and (46) into (40), and with some simple algebraic manipulations, we obtain the desired results. ■

Combining (13), (38), and (39), the AEE of a typical UE is

$$\mathrm{AEE}_{\mathrm{ue}} = \sum_{i=1}^{k} \lambda_i \int_0^{\infty} \left[\mathcal{D}_i\left(e^{\tau P_i/\bar{N}_{\mathrm{ue}}^{i}} - 1, \alpha, \{\eta_j\}\right)\right]^{-1} \mathrm{d}\tau. \tag{47}$$

Although not closed-form, the expressions of Theorem 2 are efficiently computable numerically as opposed to the Monte Carlo methods that rely on repeated random sampling to compute their results. Theorem 2 is derived by simple algebraic manipulations of Theorem 1; thus, Theorem 2 is tenable by the validation of Theorem 1.

2. Uplink Power Consumption

The power consumption of UEs is dependent on their distances from their serving BSs. Different association strategies will seriously impact this distance distribution in Lemma 1, which is closely related to uplink power consumption.

We derive the AUPC of a typical UE under the system model; that is, the association strategy and BS on-off model presented in Sections II and III. The AUPC of a typical UE is defined as

$$\mathrm{AUPC} \triangleq \mathrm{E}\left[P_{\mathrm{u}} r^{\alpha\varepsilon}\right]. \tag{48}$$

Theorem 3. For a given HetNet, the AUPC of a typical UE is

$$\mathrm{AUPC} = \frac{P_{\mathrm{u}} \Gamma\left(\frac{\alpha\varepsilon}{2} + 1\right)}{\pi^{\alpha\varepsilon/2}} \sum_{i=1}^{k} \frac{\lambda_i}{Q_i^{\left[(\alpha\varepsilon/2)+1\right]}}. \tag{49}$$

Proof. From (48),

$$\mathrm{AUPC} = \int_0^{\infty} P_{\mathrm{u}} r^{\alpha\varepsilon} f_{R_{\mathrm{s}}}(r)\,\mathrm{d}r \tag{50}$$

$$\overset{(a)}{=} 2\pi P_{\mathrm{u}} \sum_{i=1}^{k} \lambda_i \int_0^{\infty} r^{\alpha\varepsilon+1} \exp(-\pi Q_i r^2)\,\mathrm{d}r \tag{51}$$

$$\overset{(b)}{=} \frac{P_{\mathrm{u}} \Gamma\left(\frac{\alpha\varepsilon}{2} + 1\right)}{\pi^{\alpha\varepsilon/2}} \sum_{i=1}^{k} \frac{\lambda_i}{Q_i^{\left[(\alpha\varepsilon/2)+1\right]}}, \tag{52}$$

where the "(a)" in (51) is from Lemma 1 and the "(b)" in (52) follows:

$$\begin{aligned} &\int_0^{\infty} x^{\upsilon-1} \exp\left(-\mu x^{p}\right) \mathrm{d}x \\ &\quad = \frac{1}{p} \mu^{-\frac{\upsilon}{p}} \Gamma\left(\frac{\upsilon}{p}\right), \left[\mathrm{Re}\,\mu > 0, \mathrm{Re}\,\upsilon > 0, p > 0\right]; \end{aligned} \tag{53}$$

and with some simple algebraic manipulations, we obtain the desired results. ■

The validation of Theorem 3 will be verified in Section VI.

VI. Numerical Results

By giving interpretations to these results, we present the relationship between different network parameters and several system performance metrics, such as, CP, AEE, and AUPC. The results based on the traditional BSs always-on scenario [10] are also presented for comparison. Without loss of generality, we analyze the performance of a two-tier HetNet consisting of a macro tier (1st tier) and a small cell tier (2nd tier). Here, we assume the transmit powers of the macro and small cell BSs to be P_1 = 46 dBm and P_2 = 30 dBm, respectively, and the path loss exponent is assumed to be $\alpha = 4$. Furthermore, we define the offset factor $\beta = \beta_2 - \beta_1$, in the unit of dB, in the MaBRP scenario for convenience.

Figure 3 compares the probabilities of active BSs of the two -tier HetNet of Lemma 3 and the Monte Carlo simulation of the PPP model. The baseline of the traditional BSs always-on model is also shown for comparison. We observe that the approximation given in Lemma 3 is fairly accurate for MaBRP macro BS (MaMBS), MaBRP small cell BS (MaSBS), MiAD macro BS (MiMBS), and MiAD small cell BS (MiSBS). The formulae of Lemma 3 match the Monte Carlo simulation quite well. Since the macro BS and small-cell BS are equal in the MiAD mode; there is little difference in the probabilities of active BSs between MiMBS and MiSBS. Since the macro BS has a higher transmit power, more UEs will access to the macro BS in the MaBRP mode while, in the MiAD mode, the power factor is ignored. The association of UEs and their serving BSs is determined only by the distances between the UEs and their respective serving BSs; thus, MaSBS has a lower active rate than MaMBS, but this phenomenon does not happen in MiMBS and MiSBS.

Figure 4 demonstrates the results of CP from Theorem 1. A Monte Carlo simulation of the PPP model was conducted so that we could compare our analysis of the proposed model and for the purpose of model validation. We notice that the results of Theorem 1 and the Monte Carlo simulation are almost the same. It not only confirms the accuracy of Theorem 1 but also Lemma 3. The baseline, according to [10], shows an obvious gap from the Monte Carlo simulation, which means that the traditional BSs always-on model is not accurate enough for the practical network scenario, not all BSs are always active, from the point of view of SINR distribution. Furthermore, the gap between MaBRP and MiAD is obvious in a low SINR threshold region, since the user associating to the nearest BS may suffer serious interference from nearby high-power BSs. So, the MiAD is not advocated from the point of downlink coverage.

For the AEE of a typical UE versus offset factor β, demonstrated in Fig. 5, the AEE of a typical UE in MaBRP mode will increase along with an increase of the offset factor β. Since the MiAD is independent of the offset factor β, the AEE of a typical UE in MiAD mode is constant. So, from the point

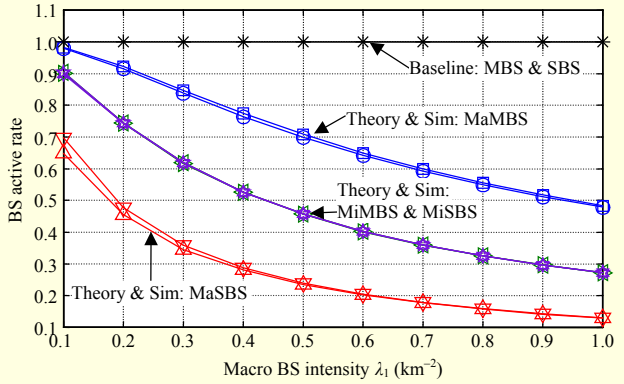

Fig. 3. Probabilities of active BSs comparison between proposed model (Lemma 3) and Monte Carlo simulation, where $\lambda_2 = 2\lambda_1$, λ_u=1 km^{-2}, and β = 2 dB (for MaBRP).

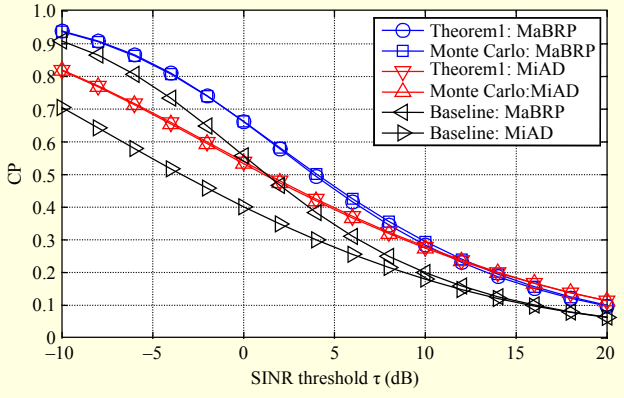

Fig. 4. CP comparison between Theorem 1 and Monte Carlo simulation of PPP, where λ_1 = 0.24 km^{-2}, $\lambda_2 = 3\lambda_1$, $\lambda_u = 3\lambda_1$, and β = 2 dB (for MaBRP).

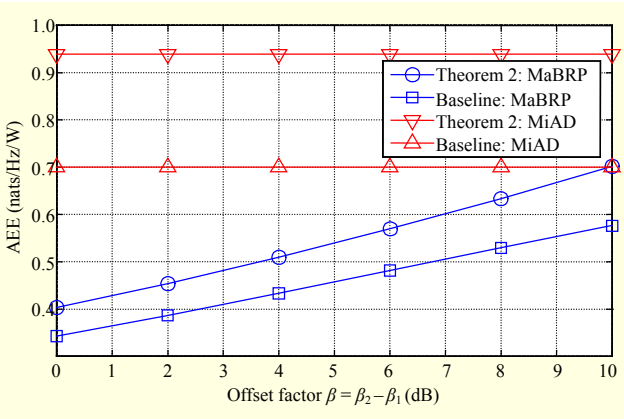

Fig. 5. AEE of a typical UE vs. offset factor β, where λ_1 = 0.24 km^{-2}, $\lambda_2 = 3\lambda_1$, and $\lambda_u = 5\lambda_1$.

ETRI Journal, Volume 37, Number 3, June 2015
http://dx.doi.org/10.4218/etrij.15.0114.0669

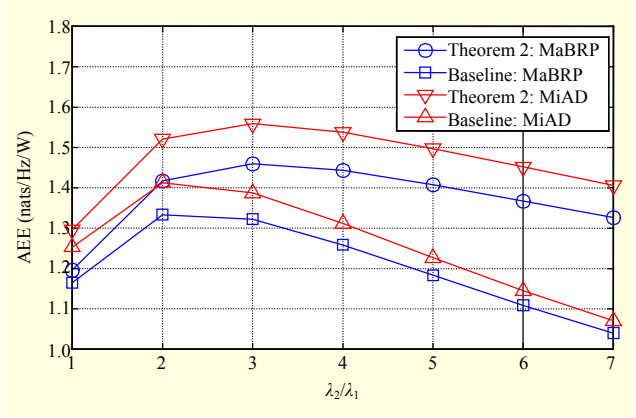

Fig. 6. AEE of a typical UE vs. λ_2/λ_1, where $\lambda_1 = 0.24$ km^{-2}, $\lambda_u = 10\lambda_1$, and $\beta = 4$ dB (for MaBRP).

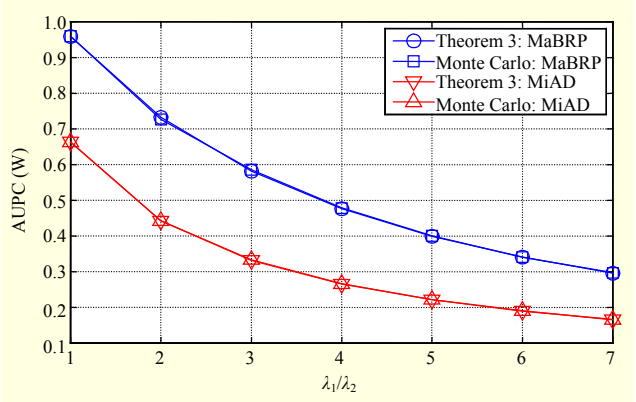

Fig. 7. AUPC comparison between Theorem 3 and Monte Carlo simulation of PPP, where $\lambda_1 = 0.24$ km^{-2}, $P_u = 1$ W, $\varepsilon = 0.5$, and $\beta = 2$ dB (for MaBRP).

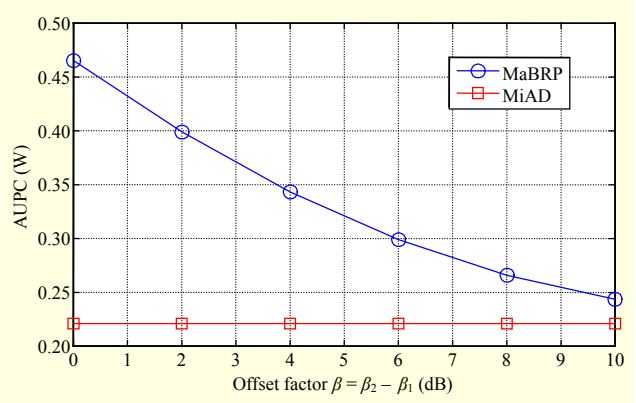

Fig. 8. AUPC of a typical UE vs. offset factor β, where $\lambda_1 = 0.24$ km^{-2}, $\lambda_2 = 5\lambda_1$, $\varepsilon = 0.5$, and $P_u = 1$ W.

of view of the AEE, range expansion is beneficial for the whole system in MaBRP mode but useless in MiAD mode. The baseline based on the traditional BSs always-on scenario is also presented for comparison. Obviously, our BS on-off model is more energy efficient in both MaBRP and MiAD. This confirms that the traditional model is not accurate enough to reflect the EE of the practical network.

For the AEE of a typical UE versus λ_2/λ_1, demonstrated in Fig. 6, the AEE will first increase and then decrease along with the increase of the density of small cells. So, we can achieve the optimal AEE by setting an appropriate density of small cells. The gap between the baseline and our BSs on-off model is noticeable, which confirms that the traditional model is not accurate enough to reflect the EE of the practical network. In addition, deploying high-density small cells will not improve the AEE, because it will reduce the average UE number of a typical cell, which will increase energy consumption per unit bit. So, from the point of view of the AEE, the deployment of too many small cells is not advocated. In addition, Figs. 5 and 6 show that the MiAD mode is more energy efficient than MaBRP.

Figure 7 demonstrates the results of the AUPC from Theorem 3 and Monte Carlo simulation of PPP. We notice that the results of Theorem 3 and Monte Carlo are almost the same. It not only confirms the accuracy of Theorem 3 but also of Lemma 1. So, we can use Theorem 3 to model and analyze the AUPC of networks. Furthermore, we can see that the AUPC will decrease with an increase to the ratio of two ties, λ_2/λ_1, as demonstrated in Fig. 7 in both MaBRP and MiAD. Along with an increase in the density of small cells, the average distance between a typical UE and its serving BS will decrease; subsequently, the transmission power consumption of the UE will decrease, since UEs utilize the distance-proportional fractional power control. The gap between MaBRP and MiAD is because the load of MiAD is more balanced than MaBRP. So, the MiAD is more beneficial in terms of the uplink power saving of UEs.

Figure 8 shows the AUPC of a typical UE versus offset factor β. For the MaBRP case, we notice that the AUPC will decrease with an increase to the offset factor β. This is because the CRE can offload the traffic from macro cells to small cells and decrease the distance from users to BSs. For the MiAD case, the AUPC does not change along with differing values of the offset factor β, because the MiAD is independent of the offset factor β. From Figs. 7 and 8, we notice that the MaBRP is more consumptive in terms of the uplink power.

VII. Conclusion and Future Work

In this paper, we developed an analytical framework for the performance evaluation of small cell networks. Different from the traditional BSs always-on model, we proposed a BSs on-off model, where a new, simple expression for the probabilities of active BSs of small cell networks (SCNs) is derived. Then,

we derived the CP, AEE, and AUPC for different association strategies, MaBRP and MiAD. The numerical results validated the analytical expressions and approximations. Our results confirm that the traditional model is not accurate enough to reflect the performance of a practical network. It is analytically shown that MaBRP is beneficial for coverage but will have some loss in energy saving. On the contrary, MiAD is not advocated from the point of coverage but is more energy efficient. The range expansion is helpful to the energy saving in MaBRP but is useless in MiAD. Furthermore, we can achieve the optimal AEE by setting an appropriate density of small cells.

In future work, we will look at combining the MaBRP and MiAD to make use of the advantages of both. Furthermore, our analytical framework for the performance evaluation of SCNs can be extended to a multi-antenna scenario.

References

[1] J.G. Andrews, "Seven Ways that HetNets are a Cellular Paradigm Shift," *IEEE Commun. Mag.*, vol. 51, no. 3, Mar. 2013, pp. 136–144.

[2] G.P. Fettweis and E. Zimmermann, "ICT Energy Consumption-Trends and Challenges," *Int. Symp. Wireless Personal Multimedia Commun.*, Lapland, Finland, Sept. 8–11, pp. 1–5.

[3] K. Son et al., "Base Station Operation and User Association Mechanisms for Energy-Delay Tradeoffs in Green Cellular Networks," *IEEE J. Sel. Areas Commun.*, vol. 29, no. 8, Aug. 2011, pp. 1525–1536.

[4] C. Li et al., "Maximizing Energy Efficiency in Wireless Networks with a Minimum Average Throughput Requirement," *IEEE Wireless Commun. Netw. Conf.*, Shanghai, China, Apr. 1–4, 2012, pp. 1130–1134.

[5] I. Christian et al., "Framework for Link-Level Energy Efficiency Optimization with Informed Transmitter," *IEEE Trans. Wireless Commun.*, vol. 11, no. 8, Aug. 2012, pp. 2946–2957.

[6] C. Xiong et al., "Energy- and Spectral-Efficiency Tradeoff in Downlink OFDMA Networks," *IEEE Trans. Wireless Commun.*, vol. 10, no. 11, Nov. 2011, pp. 3874–3886.

[7] D. Stoyan, W.S. Kendall, and J. Mecke, "*Stochastic Geometry and Its Applications*," 2nd edition, New York, NY, USA: Wiley & Sons, 1996.

[8] F. Baccelli and B. Blaszczyszyn, "*Stochastic Geometry and Wireless Networks: Volume 1 Theory*," Boston, MA, USA: Now Publishers Inc, 2010.

[9] J.G. Andrews, F. Baccelli, and R.K. Ganti, "A Tractable Approach to Coverage and Rate in Cellular Networks," *IEEE Trans. Wireless Commun.*, vol. 59, no. 11, Nov. 2011, pp. 3122–3134.

[10] H.-S. Jo et al., "Heterogeneous Cellular Networks with Flexible Cell Association: A Comprehensive Downlink SINR Analysis," *IEEE Trans. Wireless Commun.*, vol. 11, no. 10, Aug. 2012, pp. 3484–3495.

[11] S. Singh, H. Dhillon, and J.G. Andrews, "Offloading in Heterogeneous Networks: Modeling, Analysis, and Design Insights," *IEEE Trans. Wireless Commun.*, vol. 12, no. 5, May 2013, pp. 2484–2497.

[12] D. Cao, S. Zhou, and Z. Niu, "Optimal Base Station Density for Energy-Efficient Heterogeneous Cellular Networks," *IEEE Int. Conf. Commun.*, Ottawa, Canada, June 10–15, 2012, pp. 4379–4383.

[13] S. Lee and K. Huang, "Coverage and Economy of Cellular Networks with Many Base Stations," *IEEE Commun. Lett.*, vol. 16, no. 7, July 2012, pp. 1038–1040.

[14] C. Li, J. Zhang, and K.B. Letaief, "Energy Efficiency Analysis of Small Cell Networks," *IEEE Int. Conf. Commun.*, Budapest, Hungary, June 9–13, 2013, pp. 4404–4408.

[15] J. Peng, P. Hong, and K. Xue, "Stochastic Analysis of Optimal Base Station Energy Saving in Cellular Networks with Sleep Mode," *IEEE Commun. Lett.*, vol. 18, no. 4, Apr. 2014, pp. 612–615.

[16] M. Haenggi et al., "Stochastic Geometry and Random Graphs for the Analysis and Design of Wireless Networks," *IEEE J. Sel. Areas Commun.*, vol. 27, no. 7, Sept. 2009, pp. 1029–1046.

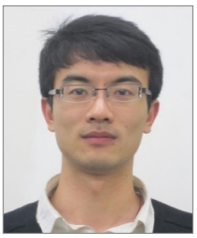

Sida Song received his BS degree in communication engineering from Beijing University of Posts and Telecommunications (BUPT), China, in July 2010. He is currently working toward his PhD degree in communication and information systems at the Wireless Theories and Technologies Laboratory, BUPT, as part of his combined MS/PhD degree program. His research interests include radio resource management in 4G wireless systems, statistical modelling of wireless networks, and stochastic geometry.

Yongyu Chang received her PhD degree in communication and information systems from Beijing University of Posts and Telecommunications, China, in July 2005. Since then, she has worked for the Wireless Theory and Technology Laboratory of School of Information and Communication Engineering, Beijing, China. She has been engaged in the research of theories and key technologies in the field of mobile communications for many years. As both a director and a key member, she has made remarkable achievements by leading or participating in many research programs, some of which are supported by the government, such as the China National 973 Program and China National 863 Program. Other programs have been company-sponsored projects. Her current research is focused on key technologies and system performance evaluations for 4G/5G wireless networks.

Xianling Wang received his BS degree in communications engineering from Beijing University of Posts and Telecommunications (BUPT), China, in 2009 and his PhD degree in communication and information systems from BUPT in 2014. He is currently a teacher at the School of Opto-Electronic and Communications Engineering, Xiamen University of Technology, China. His main research interests include multi-antenna transmissions and transmission capacity of ad hoc networks.

Dacheng Yang received his MS and PhD degrees in circuits and systems from Beijing University of Posts and Telecommunications (BUPT), China, in 1982 and 1988, respectively. From 1992 to 1993, he worked at the University of Bristol, United Kingdom, as a senior visiting scholar, where he was engaged in Project Link-CDMA of the RACE program. In 1993, he returned to BUPT as an associate professor. He is currently a professor and director of the Wireless Center of BUPT and is the prime expert of BUPT-QULACOMM, the combined research center. His current research is focused on wireless communications.